Electronic Properties of Polypyrrole/n-Si Heterojunctions and Polypyrrole/Metal Contacts

Akira Watanabe,*,† Syuuji Murakami, and Kunio Mori

Department of Applied Chemistry, Faculty of Engineering, Iwate University, Ueda, Morioka 020 Japan

Yasube Kashiwaba

Department of Electronic Engineering, Faculty of Engineering, Iwate University, Ueda, Morioka 020 Japan. *Received December 19, 1988; Revised Manuscript Received April 4, 1989*

ABSTRACT: Electronic properties of polypyrrole/n-Si heterojunctions and polypyrrole/metal contacts were investigated. Polypyrrole was electrochemically polymerized in 0.1 M pyrrole/0.05 M $(n\text{-Bu})_4NClO_4$ acetonitrile solution and polarized at various potentials to prepare samples with various contents of dopant. The sample polarized at the higher potential showed the higher content of ClO_4^- dopant and the higher spin density. The conductivity of polypyrrole increased with increasing dopant and spin density. The thermoelectromotive force suggested the characteristics of a p-type semiconductor. The I–V characteristics of polypyrrole/n-Si heterojunctions showed remarkable rectification. The contact between polypyrrole and a metal of low work function such as indium also showed rectification. These data also suggest p-type characteristics of polypyrrole. On the basis of electrical and optical data, the energy band diagrams of polypyrrole and the polypyrrole/n-Si heterojunction were discussed.

Introduction

Conductive polymers have been extensively investigated for many years because of their new properties and new conducting mechanisms. However, in the simple comparison of their bulk conductivity with metals, there are many problems for applications. Only using conductive properties in bulk phase is not effective for the new properties of conductive polymers. Recently much attention has been focused on electrochemically deposited polymers that are available as films on electrodes.[1-4] These thin films on electrodes provide many applications owing to their high conductivity and electrochemical activity.[5-7] As one interesting use, they have been investigated as a conductive coating that protects semiconductor surfaces against corrosion in photoelectrochemistry.[5,6,8] In these system, not only are properties of the bulk phase important but those of the junction interface are also quite important. With decreasing thickness of the film, the importance of junction interface increases. In the heterojunction interfaces of conductive polymer/semiconductor and contact interfaces of conductive polymer/metal, there is discontinuity of the conducting mechanism; the conductivity of polymers is explained by a quite unique mechanism, such as soliton, polaron, and bipolaron.[9] The investigations of electronic properties at the heterojunction and contact interface have just started recently.

The electronic properties of heterojunctions and contacts have been studied in the case of poly(sulfur nitride)[10] and polyacetylene.[11-13] Recently, polypyrrole/n-type semiconductor junctions and polypyrrole/metal contacts were investigated. In one case, the polypyrrole/n-Si contact was treated as a Schottky contact,[14-17] and no evidence of Schottky barrier formation was found for polypyrrole/metal of low work function contacts such as polypyrrole/Al and polypyrrole/indium contacts.[18] In other cases, well-behaved Schottky contacts were reported for polypyrrole/Al[19] or polypyrrole–poly(*N*-methylpyrrole)/indium contacts.[20] Such conflicting data are often seen in the investigation of conductive polymers because a slight difference in preparation conditions often induces different characteristics significantly. Even in the mechanism of electronic conduction of polypyrrole, there are unsolved problems.

In this paper we will report electronic properties of the polypyrrole/n-Si heterojunction and polypyrrole/metal contact and discuss the energy band diagrams of polypyrrole and the heterojunction. The characterization of polypyrrole used in our experiments was made on the basis of electrical and optical data of polypyrrole, and the electronic conduction mechanism was discussed.

Experimental Section

Materials. Pyrrole was purified by vacuum distillation. Acetonitrile was purified by distillation after dehydrogenation with diphosphorus pentaoxide. As an electrolyte in organic solvents, tetra-*n*-butylammonium perchlorate (TBAP) was used. The surface of a Pt electrode was polished with 0.3-μm Al_2O_3 powder and then rinsed with deionized water, ethanol, and trichloroethylene. The n-type Si wafer (resistivity 0.2 Ω cm) was etched in 46% aqueous HF solution for 10 s. For the spectroscopic measurements, a Pt-coated glass was used as an optically transparent electrode. Polypyrrole was prepared on a Pt electrode by galvanostatic oxidation in a 0.1 M pyrrole/0.05 M TBAP acetonitrile solution at 0.05 mA/cm^2 for 20 h. The thickness of the polypyrrole films was ca. 1.3 μm, which was estimated from the electricity passed during the electrochemical polymerization of pyrrole. The polypyrrole-coated Pt electrodes were polarized in 0.05 M TBAP at various potentials for 20 min to prepare samples with various dopant contents. The dopant density was determined by elemental analysis.

Measurements. Cyclic voltammograms were measured by a potentiostat/galvanostat (Hokuto HA-201) and a function generator (Hokuto HB-103). Electrochemical potentials were recorded versus a saturated calomel electrode (SCE). IR and near-IR spectra (8000–400 cm^{-1}) were obtained with a JEOL 100 type FT-IR spectrometer by a diffuse reflectance technique. UV and visible spectra (200–1100 nm) were measured by a Jasco Ubest-30 spectrometer with a polypyrrole-coated optically transparent electrode. ESR measurements were carried out by use of a Varian E-4 spectrometer. The spin densities were determined by use of the signal of DPPH (1,1-diphenyl-2-picrylhydrazyl) free radical as a standard. The conductivity of polypyrrole films along the surface was measured by a four-point probe method. In the measurements of the conductivity, polypyrrole films peeled from a Pt electrode were used. The conductivity in the thickness direction was measured by using sandwich cells (Pt/polypyrrole/Pt configuration). The I–V characteristics were

† Present Address: Chemical Research Institute of Non-aqueous Solutions, Tohoku University, Katahira, Sendai 980, Japan.

0024-9297/89/2222-4231$01.50/0 © 1989 American Chemical Society

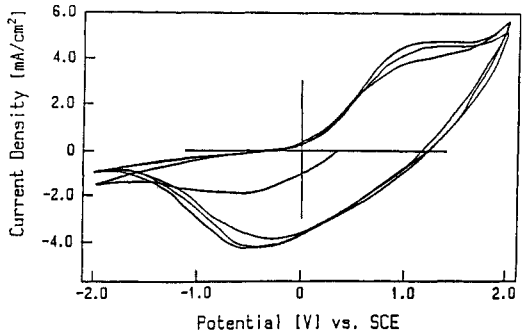

Figure 1. Cyclic voltammograms of polypyrrole in 0.05 M TBAP acetonitrile solution.

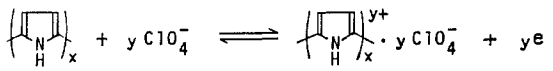

Figure 2. Redox reaction of polypyrrole.

Table I
Dopant Density and Spin Density of Polypyrrole

polarizatn potential, V	dopant density, pyrrole units/ClO_4^-	spin density	
		spins/g	pyrrole units/spin
−0.5	3.95	2.82×10^{19}	226
0.8	3.07	4.26×10^{19}	142
1.2	2.02	4.65×10^{19}	111

measured by using sandwich cells (contact area 1 cm^2), which consist of a polypyrrole-coated Pt electrode and n-Si (polypyrrole/n-Si heterojunction) or a polypyrrole-coated Pt electrode and indium (polypyrrole/indium contact). A polypyrrole on Pt electrode was contacted with n-Si or indium by interposing them between two plastic frames with rubber packing under a pressure of ca. 0.3 MPa. Ohmic contacts of leads were made for n-Si by contact with Al and for polypyrrole by contact with Pt (Pt electrode). Thermoelectromotive force was obtained by measuring the voltage difference between two probes that were 5 mm apart, one side of which can be heated. All measurements were carried out 22 °C.

Results

Electrochemical Polymerization and the Characterization of Polypyrrole. Polypyrrole has electrochemical activity[1-3] as shown in Figure 1. The electroactivity is explained by redox reaction in Figure 2. The oxidation is due to doping of ClO_4^- into the polypyrrole backbone and the reduction is due to dedoping of ClO_4^-. We prepared samples with various dopant contents by polarizing polypyrrole-coated Pt electrodes at various potentials. The dopant density for samples polarized at various potentials is shown in Table I. In organic semiconductor, dopant density does not correspond to carrier density. A possible reason for observing less radical (spin) density compared to dopant density is that the dopants tend to aggregate among themselves and therefore the number of dopant molecules that actually interact with the polymer chain can be grossly over counted. In addition the radicals may decay via cross-linking or some other mechanisms. The ESR measurements give good information on the radical sites of polypyrrole.[21] Therefore, we measured ESR spectra (Figure 3) and determined the spin density by comparison of the second integral area of the ESR spectra with that of DPPH. The spin density shows good correlation with dopant density as shown in Table I.

The optical spectrum of polypyrrole throughout the region of UV, visible, near-IR, and IR is shown in Figure 4. The abscissa in Figure 4 is indicated by electronvolt

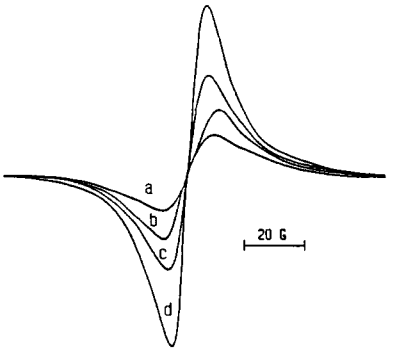

Figure 3. ESR spectra of polypyrrole polarized at various potentials: (a) −0.5 V; (b) 0.8 V, (c) 1.2 V, (d) 1.6 V. Samples, 0.5 wt % polypyrrole dispersed in KBr.

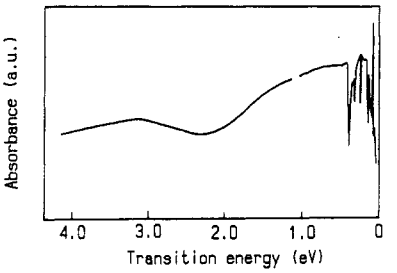

Figure 4. Absorption spectrum of polypyrrole polarized at 1.2 V.

Table II
Electric Conductivity and Activation Energy of Polypyrrole along the Surface

polariztn potential, V	σ, S/cm	ΔE, eV
−0.5	1.31	0.055
0.8	5.36	0.015
1.2	4.56	0.015

Table III
Electronic Conductivity and Activation Energy of Polypyrrole in the Thickness Direction

polarizatn potential, V	σ, S/cm	ΔE, eV
−0.5	1.11×10^{-4}	0.114
0.8	4.70×10^{-4}	0.099
1.2	7.41×10^{-4}	0.084

units to show the transition energy. Polypyrrole shows broad absorption in the near-IR and IR regions and an absorption peak around 3.1 eV.

The electric conductivity of polypyrrole films was summarized by the polarization potentials in Tables II and III. We measured electric conductivity of the film in two different directions, i.e., the conductivity along the surface direction in Table II and that in the thickness direction in Table III. There is a significant difference between them. The surface electric conductivity is higher by about 4 orders of magnitude than bulk electric conductivity. The temperature dependence of the conductivity of polypyrrole followed Arrhenius-type plots in the range between 195 and 295 K. The activation energies obtained from the slope of the plots for the conductivity along the surface and in the thickness direction are summarized in Tables II and III, respectively.

Electronic Properties of Polypyrrole/n-Si Heterojunctions and Polypyrrole/Indium Contacts. The *I–V* characteristics of polypyrrole/n-Si heterojunctions in the sandwich configuration are shown in Figure 5. The characteristics are asymmetrical and show a rectifying behavior. The forward bias corresponds to a positive voltage at polypyrrole, where holes are transferred from

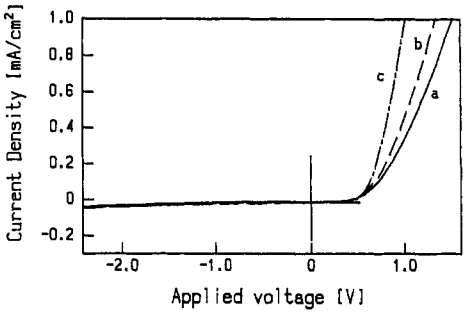

Figure 5. Current–voltage characteristics of polypyrrole/n-Si heterojunctions. Samples: polypyrrole polarized at (a) −0.5 V, (b) 0.8 V, and (c) 1.2 V.

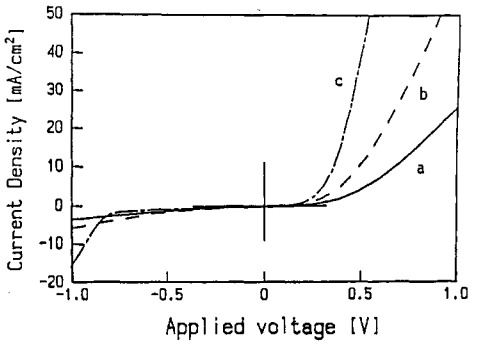

Figure 6. Current–voltage characteristics of polypyrrole/indium contacts. Samples: polypyrrole polarized at (a) −0.5 V, (b) 0.8 V; and (c) 1.2 V.

polypyrrole to n-Si and electrons are transferred from n-Si to polypyrrole. The rectification ratio (forward bias current/reverse bias current) was fairly good in three samples with different dopant contents. There is a difference in the large forward bias region higher than 0.7 V, which is the turn-on voltage. In these measurements of *I–V* characteristics, polypyrrole films prepared on Pt electrodes were used. When polypyrrole films were directly formed on n-Si electrodes in a 0.1 M pyrrole/0.05 M TBAP acetonitrile solution, good rectification characteristics could not be available because of the oxidation of n-Si in solution.

The *I–V* characteristics of polypyrrole/indium contacts are shown in Figure 6. The rectification characteristics are also shown in Figure 6. There is also a difference of the current in the large forward bias region higher than turn-on voltage because of the difference in their conductivity. Polypyrrole/Pt contacts did not show rectifying behavior and the *I–V* characteristics were symmetric in the forward and reverse voltage regions. However, the *I–V* characteristics of the contacts showed slight nonohmic characteristics in the small forward and reverse voltage regions.

Discussion

Polypyrrole films showed anisotropic conductivity as shown in Tables II and III. The conductivity along the surface (Table II) is higher by about 4 orders of magnitude than that in the thickness direction (Table III). In the measurement of *I–V* characteristics of heterojunctions and contacts, the current in the large forward bias region is controlled by the resistance in the bulk region, i.e., the conductivity in the thickness direction. We employed the conductivity in the thickness direction and the activation energy that is obtained from the temperature dependence of the conductivity (Table III) to estimate the electronic structure of polypyrrole. These activation energies, in Table III, are interpreted as the difference between the Fermi energy and valence band edge.[13] The magnitude

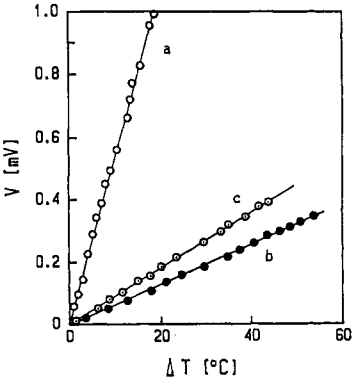

Figure 7. Thermoelectromotive force of polypyrrole polarized at various potentials. Samples: polypyrrole polarized at (a) −0.5 V, (b) 0.8 V, and (c) 1.2 V.

of these values is near 0.1 eV. The activation energy slightly decreased with increasing dopant density.

There are some possible explanations for the anisotropy in conductivity. One is that the dopants tend to remain on the surface of the film more than they penetrate into the bulk because of a diffusion barrier. Therefore, the conductivity can be much higher along the surface than in the thickness direction. The other is that the electric conductivity in the thickness direction is underestimated because of the slight nonohmic characteristics of Pt/polypyrrole/Pt contacts in the small voltage region. The conductivity along the surface could be measured by the four-point probe method, whereas this method could not be used in the measurements of the conductivity in the thickness direction and the sandwich cell Pt/polypyrrole/Pt was used. The nonohmic characteristics may be caused by the surface states on the polypyrrole surface.

Figure 4 shows broad absorption through the region of UV, visible, near-IR, and IR. There is a peak at 3.1 eV and a broad-band peak in the near-IR region. Such an absorption spectrum is typical of doped polypyrrole,[4] whereas it has been reported that neutral polypyrrole exhibits only one absorption peak at 3.2 eV.[4] This transition energy must be attributable to the bandgap of neutral polypyrrole. The broad-band absorption of doped polypyrrole must be caused by the formation of many impurity levels located in the bandgap. In our experiments, the conductivity of polypyrroles increased with increasing spin density; the spin density increased with doping ClO_4^- (Tables I and III). This suggests that the formation of radical cation sites by electrochemical oxidation (doping) increases the electronic conductivity. Such an electronic state can be explained by a polaron model.[9] The increase of absorption in the near-IR region is attributable to a polaron transition, i.e., the transition from valence band edge to polaron levels. The polaron level is a sort of impurity level.

In the case of polyacetylene, two kinds of heterojunctions have been reported; a Schottky junction between metallic AsF_5-doped $(CH)_x$ and n-type semiconductors and a p–n heterojunction between undoped p-$(CH)_x$ and n-ZnS.[12] Polyacetylene changes from a p-type semiconductor to a metal by doping. As shown in Table I, the dopant density of polypyrroles in our experiments varied by electrochemical doping–dedoping. The measurements of thermoelectromotive force provide useful information for determining the electronic state of polypyrrole.[2] Since carriers diffuse to the lower temperature side by heating one side, the lower temperature side charges positively in p-type semiconductor in which the carrier is a hole. In Figure 7, all three samples with various density of dopant show

Table IV
Barrier Height of Polypyrrole/Indium Contacts

polarizatn potential, V	ϕ_B, eV	$E_g + \chi$, eV
−0.5	0.879	5.02
0.2	0.868	5.01
0.8	0.890	5.03

Table V
Ideality Factor n and Reverse Saturation Current Density I_0 for Polypyrrole/n-Si Heterojunctions

polarizatn potential, V	I_0, A	n
−0.5	8.67×10^{-8}	9.70
0.8	5.58×10^{-7}	8.81
1.2	4.82×10^{-7}	9.29

positive thermoelectromotive force; they are p-type semiconductors.

The $I-V$ characteristics of polypyrrole/indium contacts also suggest that they are p-type semiconductors. In Figure 6, well-behaved Schottky junctions between polypyrroles and a metal of low work function (indium) are found; polypyrroles are p-type semiconductor. The current versus forward voltage characteristics can be analyzed by considering the theory of Schottky contact: $I = I_0(e^{qV/nkT} - 1)$, where I_0 is the reverse saturation current density, n the ideality factor, T the temperature, and q the magnitude of electronic charge.[22] In the low forward bias region, the characteristics are barrier controlled and the determination of I_0 and n is possible. From I_0, barrier height ϕ_B can be determined; $I_0 = A^*T^2 \exp(-q\phi_B/kT)$, where A^* is the Richardson constant, we used the value 120 A/cm^2 K^2 as the Richardson constant. Table IV shows the barrier height of polypyrrole. The values $E_g + \chi$, where E_g is the bandgap and χ is the electron affinity, can be evaluated by using the work function of indium, 4.14 eV.[13] These values are also shown in Table IV. The Fermi level of polypyrrole is ca. 0.1 eV higher than the valence band edge (Table III). Therefore, the work function of polypyrrole is ca. 4.9 eV. This value is good agreement with reported values.[14,15]

The rectification of polypyrrole/n-Si heterojunctions (Figure 5) is explained by p–n heterojunctions. The intercept and slope in current–forward voltage plots give values of reverse saturation current density I_0 and ideality factor n, respectively; $I = I_0(e^{qV/nkT} - 1)$.[23] The plots of log I versus forward voltage V in the bias region lower than turn-on voltage gave a straight line. The values of I_0 and n are summarized in Table V. The n values are significantly larger than those of inorganic semiconductors. In general, n values of inorganic semiconductors lie in the range 1–2. Such anomalous n values have also been reported on contacts of polyacetylene/metal.[13] This is due to the discontinuous structure at the interface between an organic conductor and an inorganic conductor. Furthermore, there is also discontinuity at the interface with respect to conduction mechanism. In Figure 5, there is a difference of $I-V$ curves in the large forward bias region higher than 0.7 V, which is the turn-on voltage. In the higher than turn-on voltage region, the current is controlled by the electric conductivity of the polypyrrole bulk region (Table III).[13,23]

In Figure 8, the electronic structure of polypyrrole, which is determined by electric and optical data, is shown with that of n-Si used in our experiment. Figure 8 suggests the formation of a heterojunction between polypyrrole with a wider bandgap and n-Si with narrower bandgap. The energy band diagram of the p-polypyrrole/n-Si heterojunction is depicted in Figure 9. Since the energy barrier for an electron is higher than that for a hole, the current carrier is a hole in the heterojunction.

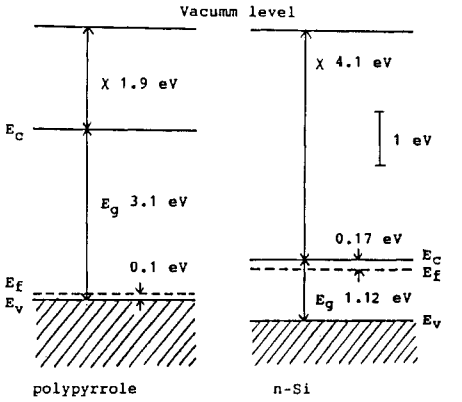

Figure 8. Energy band diagrams for isolated polypyrrole and n-Si.

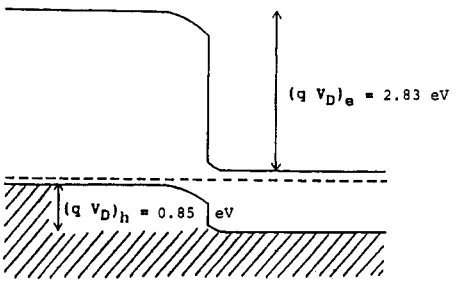

Figure 9. Energy band diagram of the polypyrrole/n-Si heterojunction at equilibrium. $(qV_D)_e$ and $(qV_D)_h$ are diffusion potentials for the electron and the hole, respectively.

Conclusion

The p-type characteristics of polypyrroles with various dopant densities were shown by the electrical and optical measurements. The conductivity of polypyrrole increased with increasing spin density, determined by ESR measurements. The measurements of the thermoelectromotive force suggested the p-type characteristics of polypyrroles. The electronic state explained by the polaron model was suggested by optical and ESR data. The $I-V$ characteristics of polypyrrole/indium and polypyrrole/n-Si showed rectifying behavior. The barrier height for the polypyrrole/indium heterojunction was determined by the analysis considering the theory of Schottky contacts. From the electrical and optical data, the energy band diagram was depicted for the polypyrrole/n-Si heterojunction. A model for typical heterojunction formed between p-polypyrrole with a wider bandgap and n-Si with a narrower bandgap was suggested.

Acknowledgment. We gratefully acknowledge the support of the Japanese Ministry of Education through a Grant-in-Aid for Developmental Science Research.

Registry No. Si, 7440-21-3; In, 7440-74-6; ClO_4^-, 14797-73-0; polypyrrole, 30604-81-0.

References and Notes

(1) Kanazawa, K. K.; Diaz, A. F.; Geiss, R. H.; Gill, W. D.; Kwak, J. F.; Logan, J. A.; Rabolt, J. F.; Street, G. B. *J. Chem. Soc., Chem. Commun.* **1979**, 845.
(2) Kanazawa, K. K.; Diaz, A. F.; Gardini, G. P.; Gill, W. D.; Grant, P. M.; Kwak, J. F.; Street, G. B. *Synth. Met.* **1980**, *1*, 329.
(3) Diaz, A. F.; Kanazawa, K. K.; Gardini, G. P. *J. Chem. Soc., Chem. Commun.* **1979**, 653.
(4) Salmon, M.; Diaz, A. F.; Logan, A. J.; Krounbi, M.; Bargon, J. *Mol. Cryst. Liq. Cryst.* **1982**, *83*, 265.
(5) Noufi, R.; Frank, A. J.; Nozik, A. J. *J. Am. Chem. Soc.* **1981**, *103*, 1849.

(6) Noufi, R.; Nozik, A. J.; White, J.; Warren, L. F. *J. Electrochem. Soc.* **1982**, *129*, 2261.
(7) Watanabe, A.; Mori, K.; Iwasaki, Y.; Nakamura, Y.; Niizuma, S. *Macromolecules* **1987**, *20*, 1793.
(8) Inganäs, O.; Lundstorn, I. *J. Electrochem. Soc.* **1984**, *131*, 1129.
(9) Bredas, J. L.; Street, G. B. *Acc. Chem. Res.* **1985**, *18*, 309.
(10) Yoshino, K.; Ura, S.; Sasa, S.; Kaneto, K.; Inuishi, Y. *Jpn. J. Appl. Phys.* **1982**, *21*, L507.
(11) Grant, P. M.; Tani, T.; Gill, W. D.; Krounbi, M.; Clarke, T. C. *J. Appl. Phys.* **1981**, *52*, 869.
(12) Ozaki, M.; Peebles, D. L.; Weinberger, B. R.; Chiang, C. K.; Gau, S. C.; Heeger, A. J.; MacDiarmid, A. G. *Appl. Phys. Lett.* **1979**, *35*, 83.
(13) Kanicki, J. *Mol. Cryst. Liq. Cryst.* **1984**, *105*, 203.
(14) Inganäs, O.; Skotheim, T.; Lundström, I. *Phys. Scr.* **1981**, *25*, 863.
(15) Inganäs, O.; Skotheim, T.; Lundström, I. *J. Appl. Phys.* **1983**, *54*, 3636.
(16) Skotheim, T.; Lundström, I.; Prejza, J. *J. Electrochem. Soc.* **1981**, *128*, 1625.
(17) Skotheim, T.; Petersson, L. G.; Inganäs, O.; Lundström, I. *J. Electrochem. Soc.* **1982**, *129*, 1737.
(18) Inganäs, O.; Lundström, I. *Synth. Met.* **1985**, *10*, 5.
(19) Kaneko, M.; Okuzumi, K.; Yamada, A. *J. Electroanal. Chem.* **1985**, *183*, 407.
(20) Koezuka, H.; Etoh, S. *J. Appl. Phys.* **1983**, *54*, 2511.
(21) Scott, J. C.; Pfluger, P.; Krounbi, M. T.; Street, G. B. *Phys. Rev. B* **1983**, *28*, 2140.
(22) Sze, S. M. *Physics of Semiconductor Devices*, 2nd ed.; John Wiley & Sons, Inc.: New York, 1981; Chapter 5.
(23) Sze, S. M. *Physics of Semiconductor Devices*, 2nd ed.; John Wiley & Sons, Inc.: New York, 1981; Chapter 2.

Monomer Concentration Effects on the Kinetics and Mechanism of the Boron Trichloride Catalyzed Solution Polymerization of Hexachlorocyclotriphosphazene

Marie Kayser Potts,* Gary L. Hagnauer, and Michael S. Sennett

Polymer Research Branch, Army Materials Technology Laboratory, Watertown, Massachusetts 02172-0001

Geoffrey Davies

Department of Chemistry, Northeastern University, Boston, Massachusetts 02115.
Received December 14, 1988; Revised Manuscript Received April 4, 1989

ABSTRACT: The boron trichloride catalyzed solution polymerization of hexachlorcyclotriphosphazene ($(NPCl_2)_3$) to poly(dichlorophosphazene) ($(NPCl_2)_n$) in 1,2,4-trichlorobenzene solution has been investigated in an attempt to elucidate its reaction mechanism. An earlier proposed mechanism involving initiation, catalysis, and inhibition by BCl_3 has been modified to account for the concentration of trimer in the reaction mixture. Reaction rates were determined by the monitoring of $(NPCl_2)_3$ concentrations with laser Raman spectroscopy and high-performance size-exclusion chromatography and by gravimetric determinations of polymer yields. Polymeric products were characterized by laser light scattering and dilute solution viscometry. Small amounts of polymer chain branching were indicated from the characterization studies.

I. Introduction

The usual method of preparing linear high molecular weight poly(dichlorophosphazene) (II) (the precursor to many poly(organophosphazenes)) is the thermal polymerization of hexachlorocyclotriphosphazene (I) (eq 1),

$$\underset{\text{I}}{(NPCl_2)_3} \xrightarrow{\Delta} \underset{\text{II}}{(NPCl_2)_n} \qquad (1)$$

generally believed to be a cationic chain growth polymerization.[1-3] Due to the high temperature required for uncatalyzed polymerization (ca. 250 °C) and the general irreproducibility of the polymerization with respect to molecular weight and cross-link content,[4,5] a great many materials have been used as catalysts to promote and control the reaction at lower temperatures.[5-7] Boron trichloride (BCl_3) is an effective catalyst for reaction 1 and leads to high yields of soluble polymer at temperatures as low as 150 °C.[8]

A previous kinetic study performed in our laboratory[9] proposed a mechanism for the boron trichloride catalyzed thermal polymerization of I in which BCl_3 acts as a polymerization initiator, catalyst for chain propagation, and a chain growth inhibitor under various conditions. However, the previous study did not examine the effects of the initial concentration of monomer, $[I]_0$, on the rates of polymerization. We have recently studied the effect of monomer concentration in 1,2,4-trichlorobenzene (TCB) solution on the polymerization rates and have modified the original proposal to account for the effects of $[I]_0$.

II. Experimental Section

Materials. Toluene and heptane were distilled from CaH_2 under N_2 and stored under N_2. Spectrophotometric grade TCB (Aldrich) and HPLC grade tetrahydrofuran (Caledon Laboratories, Ltd.) were used as received. Pentane (Caledon Laboratories, Ltd., 98.5%) was saturated with N_2 upon opening and stored under N_2. BCl_3 (C.P. grade, 99.5%) from Matheson Gas Products was used as received. Hexachlorocyclotriphosphazene was obtained from two different sources: 3PNC (99.5% pure) from Shin Nisso Kako Co., Japan, was sublimed under vacuum to remove residual solvent; Phosnic 390 (containing about 5% cyclic tetramer) from Inabata Co., Japan, was repeatedly recrystallized from heptane and sublimed. No differences were noted in the polymerization of I from the different sources.

General Polymerization Procedures. Polymerization reactions (1) were carried out in heavy-walled evacuated sealed glass tubes (25 mm o.d. × 50 mm, tapering to 5 mm o.d. × 70 mm) of approximate volume 25 mL. The smaller end of the polymerization ampule fits into the Raman spectrometer for in situ Raman measurements, while the larger end allowed larger quantities of polymer to be prepared for subsequent characterization.

In the glovebox, a flame-dried ampule was filled with approximately 10 g of a mixture of I and TCB. The tube was degassed outside the glovebox with a vacuum line and ultrasonic agitation. A measured quantity of BCl_3 (0.1–0.4 g) was condensed into the ampule by cooling with liquid nitrogen; the tube was then sealed with a flame. The tubes were subsequently heated at 200 ± 1 °C in a Fisher Iso-temp Model 350 oven.

Poly(dichlorophosphazene) (II) was isolated from the reaction tubes in the glovebox by precipitation with pentane, redissolving the precipitate in a minimum amount of toluene and precipitating again with more pentane.

0024-9297/89/2222-4235$01.50/0 © 1989 American Chemical Society